bioRxiv preprint doi: https://doi.org/10.1101/2022.10.10.511545; this version posted October 11, 2022. The copyright holder for this preprint (which was not certified by peer review) is the author/funder, who has granted bioRxiv a license to display the preprint in perpetuity. It is made available under aCC-BY-NC 4.0 International license.

MIGH-T – A Multi-Parametric and High-Throughput Platform for Host-Virus Binding Screens

Jan Schlegel[1], Bartlomiej Porebski[2], Luca Andronico[1], Leo Hanke[3], Steven Edwards[4], Hjalmar Brismar[1,4], Benjamin Murrell[3], Gerald McInerney[3], Oscar Fernandez-Capetillo[2,5], Erdinc Sezgin[1]

[1] Science for Life Laboratory, Department of Women's and Children's Health, Karolinska Institutet, 17165, Solna, Sweden

[2] Science for Life Laboratory, Division of Genome Biology, Department of Medical Biochemistry and Biophysics, Karolinska Institutet, Stockholm, Sweden.

[3] Department of Microbiology, Tumor and Cell Biology, Karolinska Institutet, Stockholm, Sweden

[4] Science for Life Laboratory, Department of Applied Physics, Royal Institute of Technology, Solna, Sweden

[5] Genomic Instability Group, Spanish National Cancer Research Centre (CNIO), Madrid, 28029, Spain.

Correspondence:

Erdinc Sezgin

Email: erdinc.sezgin@ki.se

Tel: 0046 702318248

bioRxiv preprint doi: https://doi.org/10.1101/2022.10.10.511545; this version posted October 11, 2022. The copyright holder for this preprint (which was not certified by peer review) is the author/funder, who has granted bioRxiv a license to display the preprint in perpetuity. It is made available under aCC-BY-NC 4.0 International license.

Abstract

Speed is key during infectious disease outbreaks. It is essential, for example, to identify critical host binding factors to the pathogens as fast as possible. The complexity of host plasma membrane is often a limiting factor hindering fast and accurate determination of host binding factors as well as high-throughput screening for neutralizing antimicrobial drug targets. Here we describe MIGH-T, a multi-parametric and high-throughput platform tackling this bottleneck and enabling fast screens for host binding factors as well as new antiviral drug targets. The sensitivity and robustness of our platform was validated by blocking SARS-CoV-2 spike particles with nanobodies and IgGs from human serum samples.

Main text

Emerging microbial pathogens, such as bacteria, fungi and viruses, tremendously challenge human health and cause significant economical and societal burden worldwide. Therefore, tools facilitating and improving pandemic preparedness are of uttermost importance to minimize these negative effects. Current state-of-the-art methods, such as enzyme-linked immunosorbent assay (ELISA), reverse transcription-polymerase chain reaction (RT-PCR) and RT loop-mediated isothermal amplification (RT-LAMP) usually rely on bulk measurements resulting in a single readout-value[1]. In addition, during the peaks of SARS-CoV-2 pandemic, RT-PCR instruments were used to capacity slowing down pandemic surveillance and highlighting the need for additional readout-systems. Especially flow cytometry, enabling fast and high-throughput measurements of complex mixtures, is widely used in clinics for immunophenotyping and would be an attractive and broadly available technique for such purposes[2].

To complement existing bulk measurement methods, we aimed to develop a fast and high-throughput platform. Using a bottom-up approach, we coated silica beads with a defined lipid bilayer doped with nickelated lipids. Next, we attached His-tagged host-cell proteins of interest to these membrane-coated beads to generate functionalized bead-supported lipid bilayers (fBSLBs) serving as minimal synthetic host-cells (Fig. 1a). In contrast to methods relying on random surface-adsorption, fBSLBs ensures proper protein orientation, tightly controllable receptor mobility and density as well as molecular interactions at the membrane plane (Suppl. Fig. 1). In addition, the presence of a hydrophobic lipid bilayer more closely mimics the cellular environment and enables to discriminate between binding preferences of pathogens to either host-cell proteins or lipids. For example, surface proteins of several viruses can bind different host-cell lipids facilitating cellular uptake and shaping viral tropism[3].

To validate MIGH-T, we generated fBSLBs carrying angiotensin-converting enzyme 2 (ACE2) and studied their interaction with SARS-CoV-2 spike expressing virus-like particles (+S-VLPs) using confocal microscopy (Fig.1b,c and Suppl. Fig. 2). While there was strong interaction between ACE2-fBSLBs and +S-VLPs, it was absent in VLPs with no spike (-S-VLPs) and +S-VLPs pre-treated with SARS-CoV-2 neutralizing

bioRxiv preprint doi: https://doi.org/10.1101/2022.10.10.511545; this version posted October 11, 2022. The copyright holder for this preprint (which was not certified by peer review) is the author/funder, who has granted bioRxiv a license to display the preprint in perpetuity. It is made available under aCC-BY-NC 4.0 International license.

spike nanobodies which were shown to be potent tools to neutralize SARS-CoV-2 by blocking the interaction between spike receptor-binding domain (RBD) and its host receptor ACE2[4,5]. Thus, MIGH-T can serve as powerful screening platform to identify efficient inhibitors with therapeutic potential. To increase number of data points and decrease acquisition time, we performed fast, quantitative, 3D lattice light-sheet microscopy (LLSM) and quantified viral loads per fBSLB (Fig. 1d,e) which confirmed confocal microscopy data. To screen several tens of thousands of fBSLBs within minutes, MIGH-T can be combined with fast and high-throughput flow cytometry. Individual fBSLBs were easily detected by their specific scattering signal and presence of the lipid bilayer confirmed by 1,2-dioleoyl-sn-glycero-3-phosphoethanolamine Abberior STAR RED (ASR-PE) labelling while VLPs were labelled with eGFP. Upon addition of ASR-PE and +S-VLPs to ACE2-fBSLBs, we observed a strong increase of fluorescence intensity per bead both in virus (green) and in membrane (red) channels (Fig. 1f). Moreover, virus signal decreased significantly upon nanobody treatment, confirming the neutralizing ability of nanobodies. Hence, MIGH-T enables to study host-virus interactions in a safe environment using quantitative high-throughput flow cytometry which is usually not feasible due to the small size of viral particles. Moreover, it serves as a powerful platform to study concentration-dependent effects of molecules on the binding between viruses and host-cell receptors. To show this, we determined optimal concentrations of ACE2 on the fBSLBs and the amount +S-VLPs for MIGH-T by titration series (Suppl. Fig. 3) to ensure that all nickelated lipids on the surface are bound to His-tagged host-cell receptors.

Besides ACE2, other receptors have been described to contribute to SARS-CoV-2 binding to the host-cell surface and subsequent infection. For this reason, we tested interaction of +S-VLPs with reported host-cell receptors TMPRSS2, Neuropilin-1 (CD304)[6,7], Basigin (CD147)[8], DPP4 (CD26)[9,10] and TMPRSS2[11,12] using MIGH-T. As expected, +S-VLPs showed strongest interaction with ACE2-fBSLBs (Fig. 2a). Interestingly, +S-VLPs also interacted with CD304-fBSLBs and TMPRSS2-fBSLBs, confirming that these two proteins act as host binding factors, but neither interaction was as strong as for ACE2-fBSLBs. No binding was observed for CD147-fBSLBs or CD26-fBSLBs, suggesting that these proteins cannot act as host binding factors alone and might require additional host-cell binding elements. Notably, CD304-fBSLBs binding to VLPs was independent of spike-protein on their surface, e.g., -S-VLPs also bound to CD304-fBSLBs effectively while they did not bind any other proteins we tested (Fig. 2b). This suggests the presence of another interaction partner on the (lenti) viral particles to this receptor. To check this hypothesis, we performed dual-receptor screens with each individual receptor in absence or presence of same molar concentration of ACE2 (Suppl. Fig. 5). The presence of ACE2 always significantly increased the interaction of +S-VLPs with fBSLBs, but the overall strongest binding was observed in the simultaneous presence of CD304 and ACE2, supporting the idea of two different additive binding mechanisms.

MIGH-T allows tight control not only on the composition of surface proteins but also of lipid composition. We made use of the advantage of MIGH-T to control the lipid bilayer

bioRxiv preprint doi: https://doi.org/10.1101/2022.10.10.511545; this version posted October 11, 2022. The copyright holder for this preprint (which was not certified by peer review) is the author/funder, who has granted bioRxiv a license to display the preprint in perpetuity. It is made available under aCC-BY-NC 4.0 International license.

composition and screened for reported lipid co-receptors for spike, such as GM1 gangliosides[13]. Despite varying GM1 concentrations in fBSLBs, we could not observe any concentration-dependent binding of VLPs pseudotyped with spike, beta-spike, delta-spike, Ebola virus glycoprotein (GP) or without any viral protein (Suppl. Fig. 4a,b). These results highlight the need for additional high-affinity host-cell binding factors for efficient virus-host interaction.

Key for pandemic containment is surveillance of convalescent serum samples and their ability to block the interaction between virus and host cell receptors. Virus-specific antibody levels in human serum are usually proportional to neutralization of the virus and can be used to predict disease-outcome or the need for additional booster vaccinations[14,15]. Moreover, it is very important to understand whether anti-viral IgGs in prevalent serum samples still protect from upcoming new variants to decide for vaccine-adjustments and therapeutic treatment options. To show the potential of MIGH-T to answer these questions, we first determined the amount of spike-IgGs in three human serum samples using a bead-based assay in combination with flow cytometry (Fig. 2c upper panel). Glass beads were coated with recombinant spike receptor binding domain (RBD), incubated with serum samples, and anti-spike IgGs detected by labelling with secondary dye-conjugated anti-human antibodies. After we determined the relative levels of anti-spike IgGs in the three serum samples, we blocked +S-VLPs with the different serum samples and studied the interaction with ACE2-fBSLBs by MIGH-T. The amount of anti-spike IgGs perfectly correlated with the blocking efficiency, highlighting MIGH-T's ability as powerful tool for pandemic surveillance (Fig. 2c lower panel).

Quick response to pandemic outbreaks is of uttermost importance for disease and damage control. Our platform, MIGH-T, relies on material and molecules which are available from early pandemic onset, such as the sequence of viral structural proteins and potential interaction partners. Exploiting highly specific Ni-NTA-His-tag conjugation makes the platform highly versatile and accessible, since this chemistry is widely used for protein purification and His-tagged proteins are available from a myriad of commercial resources. Screening of potential host-cell receptors and co-receptors, including lipids, can be done within a few hours using qualitative and high-throughput quantitative readout platforms. In contrast to other methods, MIGH-T enables tight control of multiple cellular parameters such as lipid composition, receptor mobility, receptor orientation, receptor-receptor interactions, and local receptor densities. The platform allows to determine serum-virus neutralization capacity in a safe laboratory environment within hours. Moreover, the presence of a lipid bilayer more closely mimics the cellular environment and can help to entangle the complex interplay between virus-receptor and virus-bilayer interactions which are often difficult to discriminate. Due to its highly defined bottom-up assembly, MIGH-T is not prone to cellular heterogeneity, e.g. due to differences in cell-cycle states, transcription and translation, which can complicate drug screens. Our broadly accessible platform enables to perform fast and high-throughput drug screens and to discriminate whether drugs act on the virus particles or on the host-cell receptors. Due to its bottom-up

bioRxiv preprint doi: https://doi.org/10.1101/2022.10.10.511545; this version posted October 11, 2022. The copyright holder for this preprint (which was not certified by peer review) is the author/funder, who has granted bioRxiv a license to display the preprint in perpetuity. It is made available under aCC-BY-NC 4.0 International license.

design, MIGH-T should be readily extensible to other biomolecules (e.g. glycocalyx, DNA, RNA) and pathogens (bacteria, fungi) making it a valuable tool for future pandemic preparedness.

Materials and Methods

fBSLB preparation

For preparation of one batch of fBSLBs, $1x10^7$ 5µm silica beads (Bangs Laboratories) were vortexed thoroughly and washed three times with PBS using 1500xg and 30 seconds centrifugation steps. Beads were coated with lipid bilayers of defined compositions by incubation with 100µl 0.5mg/ml liposomes shaking at 1400rpm for 30 minutes. Liposomes were formed by mixing lipids dissolved in chloroform, solvent evaporation under a steam of nitrogen, re-hydration, and tip-sonication (Branson Sonifier 250). To prepare fBSLBs with His-tagged proteins, a lipid mixture consisting of 98mol% POPC and 2mol% 18:1 DGS-Ni:NTA (Avanti Polar Lipids) was used. After bilayer formation beads were washed two more times with PBS and 5pmol of His-tagged proteins added (Sino Biological: ACE2-His 10108-H08H, Neuropilin-1-His 10011-H08H, CD147-His 10186-H08H, CD26-His 10688-H08H). After 20 minutes on a rotary shaker the bilayer of fBSLBs was optionally directly labelled with a fluorescent lipid analogue followed by 2 washing steps with PBS. Final fBSLBs were diluted in 500µl PBS and used the same day. To study host-virus interactions, 20µl of fBSLBs were mixed with 15µl of GFP-tagged pseudotyped VLPs and incubated for 30 minutes on a rotary shaker at room temperature and directly used for microscopy or flow cytometry. Optionally, VLPs were pre-treated for 20 minutes on ice with 2µM Ty1, Ty1-Fc or Fu2 nanobodies[4,5].

VLP preparation

Mycoplasma-free HEK293T cells were cultured in DMEM supplemented with 10% FCS and grown to ~70% confluency in T75 cell culture flasks. To produce VLPs, cells were co-transfected using Lipofectamine 3000 and 15µg of DNA encoding for viral protein (pCMV14-3X-Flag-SARS-CoV-2 S was a gift from Zhaohui Qian - Addgene plasmid # 145780; delta/beta spike expression plasmid kindly provided by Benjamin Murrell; Ebola GP expression plasmid kindly provided by Jochen Bodem), 7.5µg DNA encoding for HIV Vpr-GFP (NIH HIV Reagent Program, Division of AIDS, NIAID, NIH: pEGFP-Vpr, ARP-11386, contributed by Dr. Warner C. Greene), and 7.5µg encoding for a lentiviral packaging plasmid (psPAX2 was a gift from Didier Trono - Addgene plasmid # 12260). Media was exchanged after 12 hours and VLPs harvested after 24 and 48 hours and enriched fiftyfold using LentiX concentrator according to the protocol provided by the manufacturer (Takara).

Microscopy and Quantification

After incubation with pseudotyped VLPs, fBSLBs were put into chambered glass coverslips (IBIDI: 81817) and imaging performed in PBS. Confocal microscopy was performed using a C-Apochromat 40x/1.20 water immersion objective of the Zeiss

bioRxiv preprint doi: https://doi.org/10.1101/2022.10.10.511545; this version posted October 11, 2022. The copyright holder for this preprint (which was not certified by peer review) is the author/funder, who has granted bioRxiv a license to display the preprint in perpetuity. It is made available under aCC-BY-NC 4.0 International license.

LSM780 microscope. Viral GFP was excited using 488nm argon laser and membrane-inserted ASR-PE was excited using a 633nm helium neon laser, while emission was collected from 498-552nm and 641-695nm, respectively. Full surface of 5µm fBSLBs was recorded by acquiring z-stacks with 24 slices each 0.3µm and VLP-GFP signal per bead quantified using ImageJ following the provided macro and automated workflow of Suppl. Fig. 02. To acquire fast, gentle, and big 3D volumes we used LLSM (Zeiss Lattice Lightsheet 7) with 488nm and 640nm laser excitation for viral GFP and ASR-PE, respectively. The general analysis workflow followed the one for confocal data, but parameters were adjusted for differences in signal intensity.

Flow Cytometry

Upon interaction of VLPs with fBSLBs the mixture was diluted in 500µl PBS and transferred into flow tubes. Flow cytometry was performed using a BD Fortessa system acquired at low speed and 488nm (FITC) or 640nm (APC) excitation/emission settings used for VLP-GFP and ASR-PE, respectively. 10 000 to 20 000 events were acquired and analysed using FCS Express 7 and Python (FCSParser). Gating was only performed for data shown in Fig. 1f on singlet bead population clearly visible in the forward- versus side-scatter plot. This population was always at least 85% of the total bead population.

Serum Blocking

Human blood from healthy donors was obtained from blood transfusion station of Karolinska Hospital and serum prepared by centrifugation. The serum was aliquoted and frozen for further later use. To determine the amount of anti-spike IgGs in serum samples, $1x10^7$ 5µm silica beads (Bangs Laboratories) were washed three times with PBS and coated for 30 minutes with 47pmol SARS-CoV-2 RBD (BioSite: 40592-V08H) on a rotary shaker. After two washing steps with PBS beads were resuspended in 500µl PBS supplemented with 4mg/ml BSA to block non-specific interaction sites. 20µl of beads were incubated with stated serum dilutions over night at 4°C on a rotary shaker to enable interaction of anti-spike IgGs with coated beads. After two washing steps, anti-spike IgGs were labelled by incubation with 4µg/ml secondary anti-human IgG Alexa Fluor 488 antibodies (ThermoFischer: A11013) for one hour at room temperature on a rotary shaker in the dark. Labelled beads were washed and signal intensity of at least 9000 beads determined by flow cytometry. To test serum blocking efficiency, VLPs were pre-treated with stated serum concentrations over night at 4°C on a rotary shaker before incubated with ACE2-fBSLBs as described above.

Acknowledgements

This work was supported by the National Microscopy Infrastructure, NMI (VR-RFI 2016-00968) and grants from the SciLifeLab National COVID-19 Research Program, financed by the Knut and Alice Wallenberg Foundation. This project has received funding from the European Union's Horizon 2020 research and innovation program under grant agreement No. 101003653 (CoroNAb), to B.M. and G.M. We thank Jaromir Mikes for support with flow cytometry. We acknowledge the G2P-UK National

bioRxiv preprint doi: https://doi.org/10.1101/2022.10.10.511545; this version posted October 11, 2022. The copyright holder for this preprint (which was not certified by peer review) is the author/funder, who has granted bioRxiv a license to display the preprint in perpetuity. It is made available under aCC-BY-NC 4.0 International license.

Virology consortium funded by MRC/UKRI (grant ref: MR/W005611/1.) and the Barclay Lab at Imperial College for providing the plasmids Beta/B.1.351 and Delta/B.1.617.2.

Data availability statement

All raw data will be available upon publication (FigShare DOI: 10.17044/scilifelab.20517336).

References

1. Kevadiya, B. D. *et al.* Diagnostics for SARS-CoV-2 infections. *Nat. Mater.* **20**, 593–605 (2021).
2. Maecker, H. T., McCoy, J. P. & Nussenblatt, R. Standardizing immunophenotyping for the Human Immunology Project. *Nat Rev Immunol* **12**, 191–200 (2012).
3. Mazzon, M. & Mercer, J. Lipid interactions during virus entry and infection: Lipids and Viruses. *Cell Microbiol* **16**, 1493–1502 (2014).
4. Hanke, L. *et al.* An alpaca nanobody neutralizes SARS-CoV-2 by blocking receptor interaction. *Nat Commun* **11**, 4420 (2020).
5. Hanke, L. *et al.* A bispecific monomeric nanobody induces spike trimer dimers and neutralizes SARS-CoV-2 in vivo. *Nat Commun* **13**, 155 (2022).
6. Cantuti-Castelvetri, L. *et al.* Neuropilin-1 facilitates SARS-CoV-2 cell entry and infectivity. *Science* **370**, 856–860 (2020).
7. Daly, J. L. *et al.* Neuropilin-1 is a host factor for SARS-CoV-2 infection. *Science* **370**, 861–865 (2020).
8. Wang, K. *et al.* CD147-spike protein is a novel route for SARS-CoV-2 infection to host cells. *Sig Transduct Target Ther* **5**, 283 (2020).
9. Vankadari, N. & Wilce, J. A. Emerging COVID-19 coronavirus: glycan shield and structure prediction of spike glycoprotein and its interaction with human CD26. *Emerging Microbes & Infections* **9**, 601–604 (2020).
10. Li, Y. *et al.* The MERS-CoV Receptor DPP4 as a Candidate Binding Target of the SARS-CoV-2 Spike. *iScience* **23**, 101160 (2020).
11. Hoffmann, M. *et al.* SARS-CoV-2 Cell Entry Depends on ACE2 and TMPRSS2 and Is Blocked by a Clinically Proven Protease Inhibitor. *Cell* **181**, 271-280.e8 (2020).
12. Hussain, M. *et al.* Molecular docking between human TMPRSS2 and SARS-CoV-2 spike protein: conformation and intermolecular interactions. *AIMS Microbiology* **6**, 350–360 (2020).

bioRxiv preprint doi: https://doi.org/10.1101/2022.10.10.511545; this version posted October 11, 2022. The copyright holder for this preprint (which was not certified by peer review) is the author/funder, who has granted bioRxiv a license to display the preprint in perpetuity. It is made available under aCC-BY-NC 4.0 International license.

13. Nguyen, L. *et al.* Sialic acid-containing glycolipids mediate binding and viral entry of SARS-CoV-2. *Nat Chem Biol* **18**, 81–90 (2022).
14. Khoury, D. S. *et al.* Neutralizing antibody levels are highly predictive of immune protection from symptomatic SARS-CoV-2 infection. *Nat Med* **27**, 1205–1211 (2021).
15. Bates, T. A. *et al.* Neutralization of SARS-CoV-2 variants by convalescent and BNT162b2 vaccinated serum. *Nat Commun* **12**, 5135 (2021).

bioRxiv preprint doi: https://doi.org/10.1101/2022.10.10.511545; this version posted October 11, 2022. The copyright holder for this preprint (which was not certified by peer review) is the author/funder, who has granted bioRxiv a license to display the preprint in perpetuity. It is made available under aCC-BY-NC 4.0 International license.

Figures

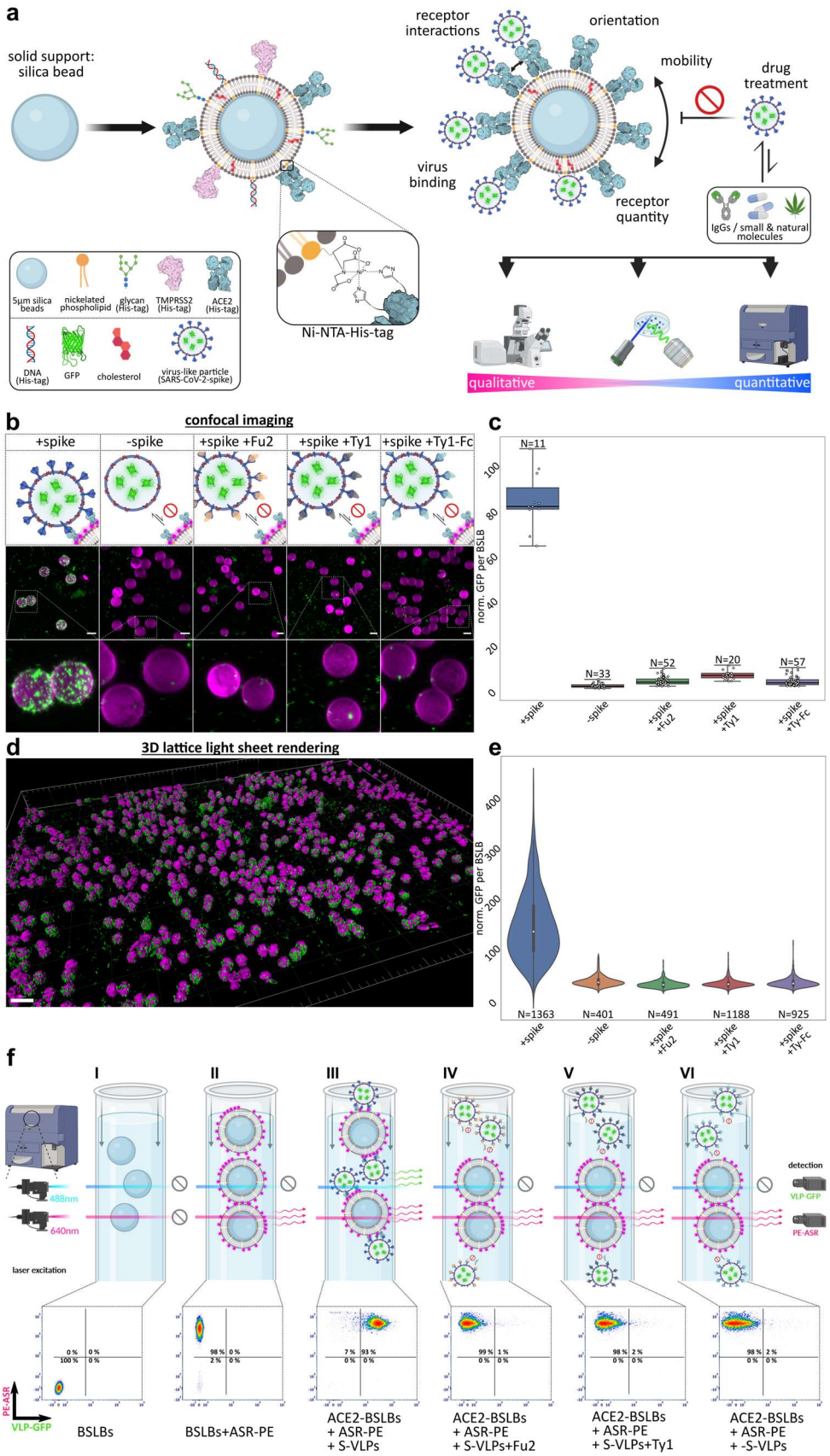

bioRxiv preprint doi: https://doi.org/10.1101/2022.10.10.511545; this version posted October 11, 2022. The copyright holder for this preprint (which was not certified by peer review) is the author/funder, who has granted bioRxiv a license to display the preprint in perpetuity. It is made available under aCC-BY-NC 4.0 International license.

Figure 1: Design and characterization of our multi-parametric and high-throughput platform MIGH-T, based on fBSLBs to study host-virus interactions. (a), Scheme depicting the bottom-up assembly of fBSLBs and available readout techniques. (b), LSM maximum-intensity projections of BSLBs (magenta) and VLPs (green) showing specific interaction between SARS-CoV-2 spike VLPs (+S-VLPs) and ACE2-fBSLBs. (c) Quantification of viral GFP-signal per fBSLBs of each condition from (b) shows specific attachment of +S-VLPs to ACE2-fBSLBs (median=84.05 , N=11) and no interaction between -S-VLPs and ACE2-BSLBs (median=2.88 , N=33) and nanobody-pretreated +S-VLPs and ACE2-BSLBs (Fu2: median=4.70 , N=52 ; Ty1: median=7.77 , N=20 ; Ty-Fc: median=4.41 , N=57). Boxplot with overlay of individual data points, median as black center line, box showing the quartiles and whiskers from minimum to maximum value. (d) Fast and quantitative LLSM enabling big-volume renderings of ACE2-fBSLBs (magenta) interacting with +S-VLPs (green). (e) Quantification of VLP-GFP signal per bead proves specific interaction between +S-VLPs and ACE2-fBSLBs (N>400). Violinplot with miniature boxplot showing quartiles and median as white dot. (f) Fast high-throughput screening of interaction between VLPs and ACE2-fBSLBs using flow cytometry. Strong signal of the fluorescent lipid ASR-PE (y-axis) confirms functional bilayer formation and interaction of VLPs with fBSLBs can be followed by intensity changes in the VLP-GFP channel (x-axis) (N>8500 per condition). Illustrations were created using Biorender.com and Inkscape.

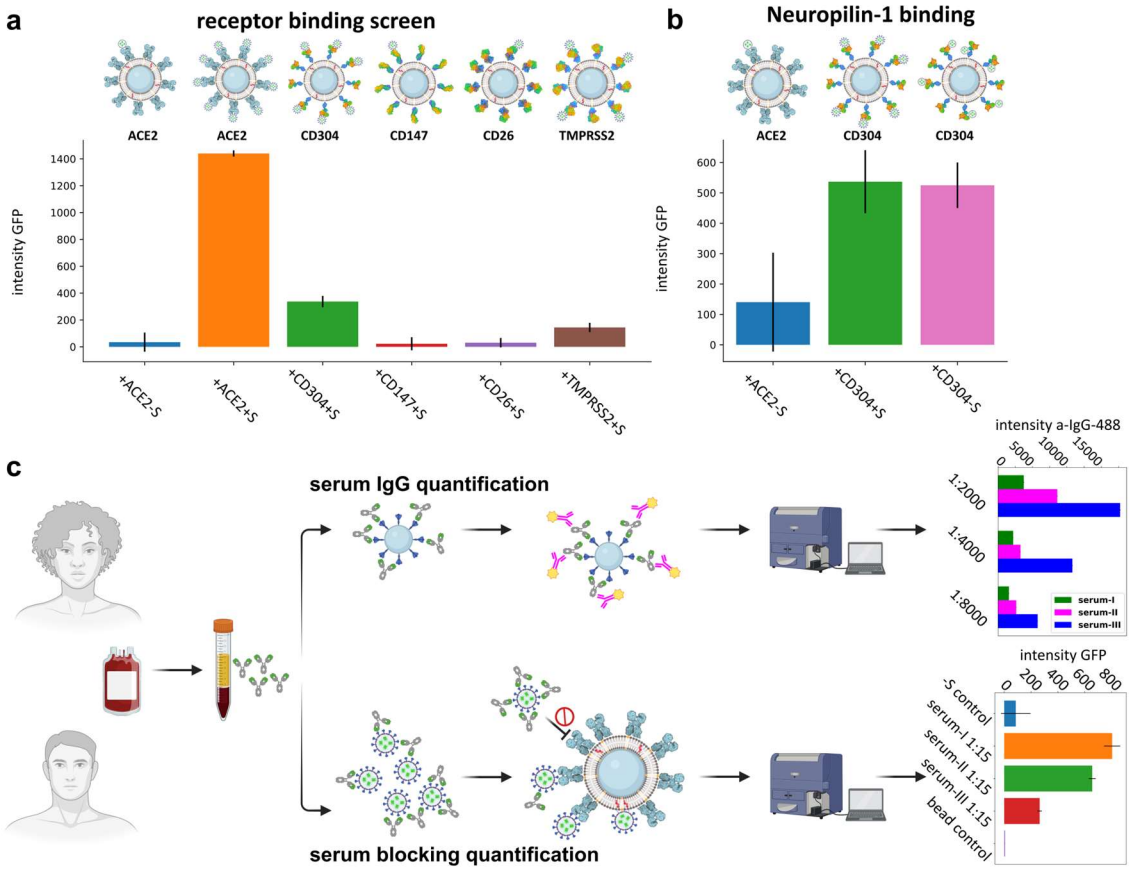

Figure 2: Application of MIGH-T to study interaction with different host-receptors and the neutralizing antibodies in human blood serum samples. (a) Scheme depicting fBSLBs with different His-tagged host-receptors. Bar graphs showing the median ± standard error of median of +S-VLP-GFP signal of 40000 BSLBs analyzed by flow cytometry. Besides ACE2, specific but less pronounced binding was also observed for CD304 and TMPRSS2. (b) MIGH-T identified interaction of VLPs with CD304-fBSLBs even in the absence of spike protein (N=20000). (c) Scheme showing the processing of human serum samples to quantify amount of anti-spike IgGs and their capacity to block the interaction between +S-VLPs and ACE2-fBSLBs. Upper bar graphs illustrating the amount of anti-spike IgGs in three different serum samples at different dilutions (N=10000). Lower bar graphs showing the efficiency to block the

bioRxiv preprint doi: https://doi.org/10.1101/2022.10.10.511545; this version posted October 11, 2022. The copyright holder for this preprint (which was not certified by peer review) is the author/funder, who has granted bioRxiv a license to display the preprint in perpetuity. It is made available under aCC-BY-NC 4.0 International license.

interaction between +S-VLPs and ACE2-BSLBs for the three different serum samples as illustrated by the median ± standard error of each population (N=10000). Note that the amount of anti-spike-IgGs in the serum samples correlates with blocking efficiency. Illustrations were created using Biorender.com and Inkscape.